Photoconductivity and Performance of Mn^{2+} and Ce^{3+} Doped ZnS Quantum Dot Detectors

The 5th International scientific Conference on Nanotechnology& Advanced Materials Their Applications (ICNAMA 2015)3-4 Nov, 2015

Dr. Raad M.Al-Haddad
College of Science, University of Baghdad, Baghdad
Email: rahaddad61@yahoo.com
Dr. Iftikhar M.Ali
College of Science, University of Baghdad, Baghdad**.**
Dr. Issam M. Ibrahim
College of Science, University of Baghdad, Baghdad
Dr. Naser M. Ahmed
School of Physics, University Science Malaysia , Malaysia

ABSTRACT

Mn^{2+} and Ce^{3+} Doped ZnS nanocrystals were prepared by a simple microwave irradiation method under mild condition. The starting materials for the synthesis of Mn^{2+} and Ce^{3+} Doped ZnS P nanocrystals were zinc acetate as zinc source, thioacetamide as a sulfur source, manganese chloride and Cerium chloride as manganese and cerium sources respectively (R & M Chemical) and ethylene glycol as a solvent. All chemicals were analytical grade products and used without further purification. The nanocrystals of Mn^{2+} and Ce^{3+} Doped ZnS P with cubic structure were characterized by X-ray powder diffraction (XRD), the morphology of the film is seen by field effect scanning electron microscopy (FESEM). The composition of the samples is analyzed by EDS. The spectral response of Mn^{2+} and Ce^{3+} Doped ZnS nanocrystals was studied. The values of responsively, specific detectivity and quantum efficiency for Ce^{3+} Doped ZnS are higher than that for Mn^{2+} Doped ZnS.
Keywords: Photoconductivity, Zinc Sulfide, Quantum Dots, datectors, Microwave Irradiation.

التوصيلية الضوئية وأدائية كواشف كبريتيد الزنك المطعمة بالمنغنيز والسيريوم
الخلاصة

تم تحضير النقاط الكمية للمركب كبريتيد الزنك المطعم بعنصري المنغنيز والسيريوم بالطريقة الكيميائية تحت اشعاع الموجات المايكروية . المواد الاولية لتحضير المركب المطعم هي خلات الزنك كمصدر لعنصر الزنك والثايواسيتمايد كمصدر لعنصر الكبريت كما استخدم كلوريد المنغنيز وكلوريد السيريوم كمصدرين لكل من المنغنيز والسيريوم على التوالي، والماء الممزوج بالاثيلين كلايكول كمذيب. تم تشخيص تركيب المركب المطعم بواسطة حيود الاشعة السينية وتبين انه ذو تركيب مكعب، ماهية السطح للاغشية المحضرة قد تم فحصها باستخدام انبعاث المجال للمجهر الالكتروني الماسح. تم تحليل مكونات الاغشية بواسطة مطياف طاقة التشتت. وقد درست الاستجابة الطيفية للمركب المطعم واتضح ان الاستجابة والكشفية النوعية والكفاءة الكمية لمركب كبريتيد الزنك المطعم بالسيريوم هي افضل من تلك التي للمركب المطعم بالمنغنيز

INTRODUCTION

Nanocrystal (NC) is defined as a cluster that contains from a few hundred to tens of thousands of atoms, ranging anywhere from a couple of nanometers to tens of nanometers in size. Nanocrystals are very attractive and interesting because they have unique properties that set them apart from typical bulk materials. These unique properties result because nanocrystals are larger than molecules, but much smaller than bulk materials. As a result, nanocrystals show properties that are somewhere in between the properties of discrete molecules and bulk materials [1]. When the size or shape of nanocrystals is changed, their properties can also be altered accordingly, enabling scientists to tune them for specific purposes. In addition, it is easy to grow flawless, perfect nanocrystals since their length of scale is so small that there is barely any time to introduce defects [2,3]. Because of these reasons, much investigation is dedicated to the study of nanocrystals and how their special properties can be applied to practical applications.

Photoconductivity (PC) is defined as electrical conductivity resulting from photo-induced electron excitations in which light is absorbed. In semiconductors, photoconductivity arises due to interaction of photons with bound electrons of lattice atoms that leads to photo-generation of electron-hole pairs after absorption of photons which increases carrier density and conductivity of material [4,5]. Extensive study of photoconductivity has been made in nanoparticles, thin film, nanorods, nanowires and mixed lattice [6-8] for different parameters.

Wide-bandgap II–VI compounds have been applied to optoelectronic devices, especially light emitting devices in the short-wavelength region of visible light. Here our focus is on ZnS semiconductor which is studied in the present study. Zinc sulfide (ZnS) is one of the most typical and important crystalline materials for both application and research [1,9]. Research studies are carried out on doped II-VI semiconductor nanomaterials to enhance their light emission properties and thereby making them good candidate for optoelectronic applications such as displays, sensors and lasers. The doping of ZnS with transition metals such as Mn, and rare earth such as Ce is interesting to researchers because of the effect of dopant on the photoluminescence and photoreactivity properties of the semiconductor [10,11,12].

EXPERIMENTAL

The starting materials for the synthesis of Mn and Ce doped ZnS NCs were zinc acetate as zinc source, thioacetamide as a sulfur source, manganese chloride and Cerium chloride as manganese and cerium sources respectively and ethylene glycol mixed with distilled water as a solvent. In a typical synthesis, 5 mM of zinc source and 0.05mM of manganese or cerium source were added with appropriate concentrations of Manganese or cerium (1wt.%) in a glass beaker of 80 mL containing 20 mL of ethylene glycol and 60ml distilled water as solvent . The solution was stirred for 1hour at $70^{oP}C$, and then 6 mM of sulfur source dissolved in 20ml was added by drop wise and stirred for 30 min. The beaker was placed in a high power microwave oven (1100 W) operated using a pulse regime with 20% power for 25 min irradiation time. The formed precipitates were centrifuged (4000 rpm, 10 min) and the residue was washed several times with distilled water and absolute ethanol. The products were dried in air at 60°C for 24 h under control environment and can be stored for extended period of time.

Results and discussion
Structural Analysis:
XRD Analysis for Mn²⁺ and Ce³⁺ Doped ZnS QDs

The XRD patterns of Mn²⁺ and Ce³⁺ Doped ZnS QDs are displayed in Fig.1. It can be identified as the cubic zinc blende structure with a comparison to the standard card (JCPDS, no. 05-0566). As seen from Fig.1, the diffraction peaks from (111), (220), and (311) planes have appeared in the XRD patterns. The data of structural parameters are shown in Table-1.
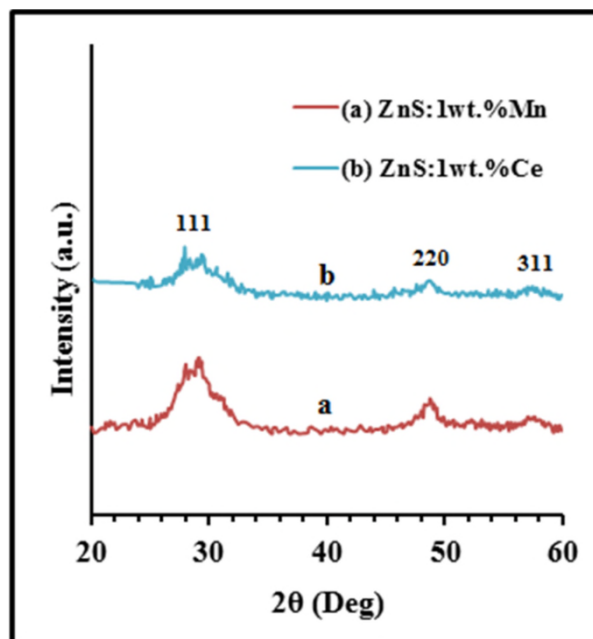
Figure(1) XRD patterns for(a) ZnS:1wt.%Mn QDs and (b) ZnS:1wt.%Ce QDs.
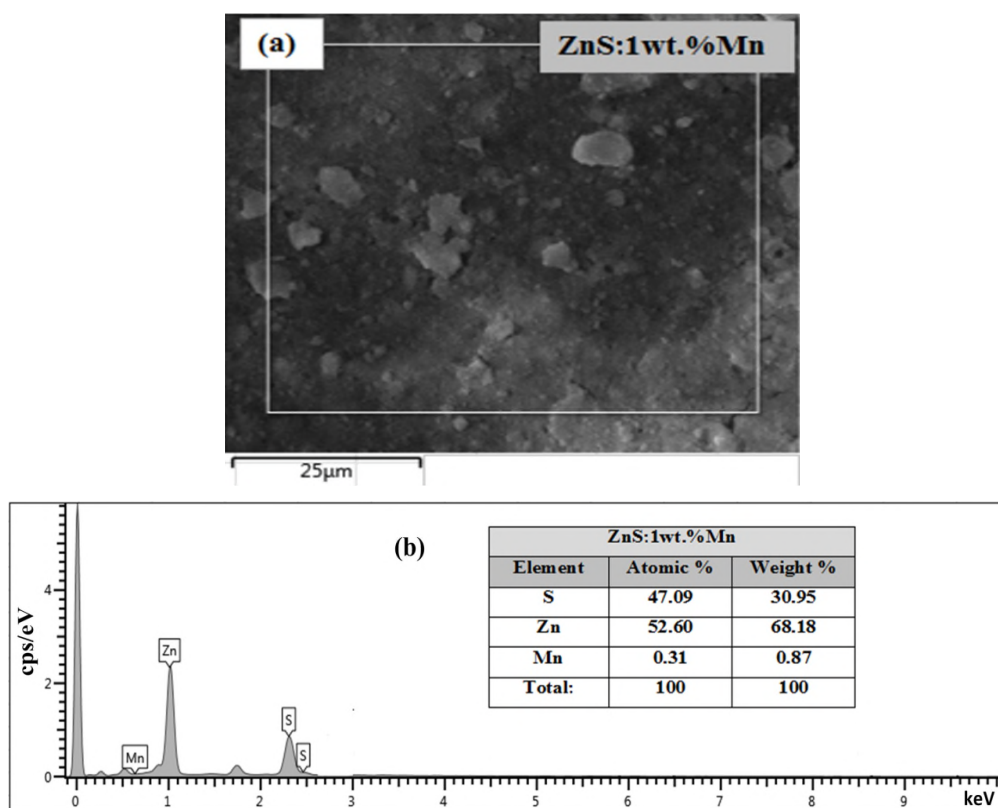
The crystallite sizes are calculated from Scherrer equation $D=K\lambda/(\beta\cos\theta)$ [13] to be (3.56 and 1.14) nm for Mn²⁺ and Ce³⁺ Doped ZnS QDs respectively, i.e. the radii are (1.78 and 0.57) nm, which is smaller than Bohr radius a_B , where Bohr radius for ZnS is 2.5nm, so our samples have radii smaller than Bohr radius. That means, we have quantum dot (QD) nanocrystals. So we have strong confinement in the wave function of the electron. Also, we can see that the size of Ce³⁺ Doped ZnS QDs is smaller than that for Mn²⁺ and Doped ZnS QDs, and this is very clear from the broadening of the diffraction peaks in (Fig. 1b), also FWHM data in Table-1 for Ce³⁺ Doped ZnS are larger than that for Mn²⁺ Doped ZnS. So that the surface area to volume ratio is higher with Ce³⁺ Doped ZnS QDs.

Table (1) Structural Parameters of Mn^{2+} and Ce^{3+} Doped ZnS QDs which are diffraction angle (2θ), (hkl), d-spacing, and FWHM.
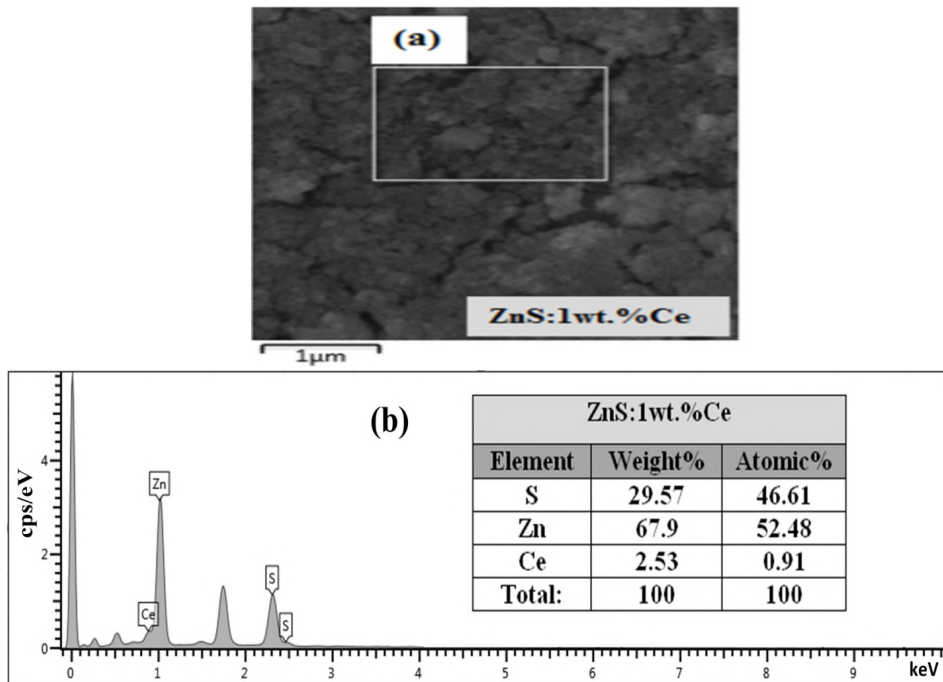
Sample	2θ (Deg)	Plane (hkl)	Interplaner Spacing d(A⁰)	FWHM (rad)	Lattice constant a(Å)	Average Crystallite Size D (nm)
ZnS:2wt.%Mn	28.8440	(111)	3.09281	0.0309	5.3635	3.56
	48.0492	(220)	1.89203	0.0287		
	56.8629	(311)	1.61791	0.0257		
ZnS:2wt.%Ce	29.1445	(111)	3.06160	0.0776	5.2559	1.14
	47.0608	(220)	1.92944	0.0514		
	57.4391	(311)	1.60304	0.0297		

EDS Analysis for Mn^{2+} and Ce^{3+} Doped ZnS QDs

The chemical composition of the samples is analysed by EDS. Figures 2 & 3 proved the presence Zn, S with small traces of Mn^{2+} and Ce^{3+}ions as depicted in the spectra. The concentration of dopants is normally too small to detect with EDS, but in this case a very small Mn and Ce peaks are observed suggesting that the amount of Mn and Ce present in the synthesized compound is high (> 1 wt %).

Figure(2)(a) SEM image for ZnS:1wt.%MnQDs, (b) EDS spectrum for ZnS:1wt.%MnQDs

ZnS:1wt.%Ce		
Element	Weight%	Atomic%
S	29.57	46.61
Zn	67.9	52.48
Ce	2.53	0.91
Total:	100	100

**Figure(3)(a) SEM image for ZnS:1wt.%Ce, (b) EDS spectrum for ZnS:1wt.%Ce
b) Morpgology of Mn²⁺ and Ce³⁺ Doped ZnS QDs.**

FESEM Analysis for Mn²⁺ and Ce³⁺ Doped ZnS QDs

Figures 4 & 5 illustrate FESEM images of Mn²⁺ and Ce³⁺ Doped ZnS films, respectively, at low and high magnifications. It is obvious that the prepared nanoparticles were found to be in cluster form. The surface morphology of doped ZnS QDs have spherical shape. In some places, various sizes of the particles (small and large size) are observed, i.e. nano-sized particles seem to be randomly distributed in the films and this observation also has been seen by Kanazawa and Kamitani [14].
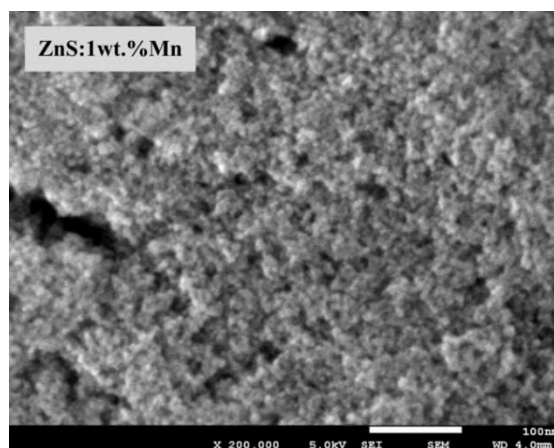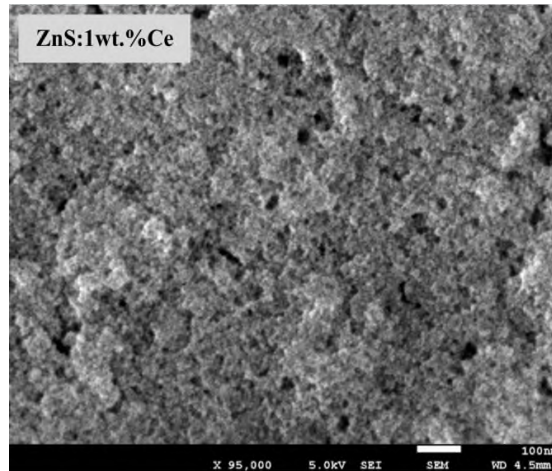

Figure (4)FESEM images of ZnS:1wt.%Mn QDs

Figure(5) FESEM image of Ce doped ZnS QDs

## Photoconductivity study for Mn²⁺ and Ce³⁺ Doped ZnS QDs

(I-t) characterization of our optoelectronic devices and the performance such as figure of merit of the photodetector have been studied.

(I-t) characteristic for Mn²⁺ and Ce³⁺ Doped ZnS QDs photoconductor device

When the light was turned on, conductivity increased and after the light was turned off, the current returned to its original value. This process was repeated many times as seen from Figures (6&7). From our data, it appears to be possible to control the response of the current in a semiconducting photodetector because the electrons in the nanoparticles receive their excitation energy from the power of the light source, it is possible to "switch" these nanoparticles reversibly between higher and lower states of conductivity. As we see from the current an average of ~ ms rise time τ_r to travel from its lowest point to its highest and nearly ~ ms fall time τ_f to retreat once the light was turned off. This response rate is fast, especially for an electronic device. The gain **G which is I_{ph}/I_d** and Sensitivity equals to **[Gx100%]** are listed in Table-2.
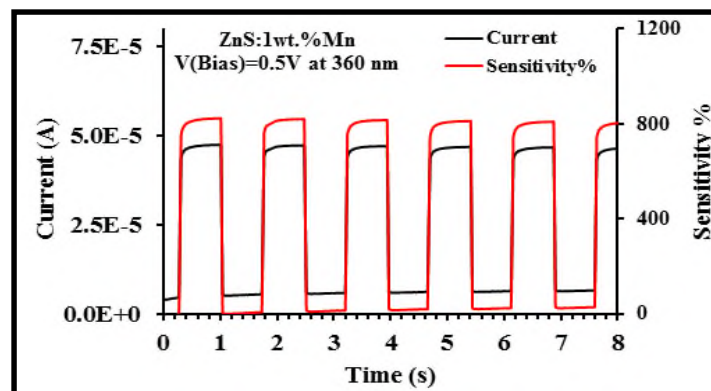
Figure(6) Photoresponse time of the fabricated ZnS:1wt.%Mn QDs UV photodetector upon exposure to 360nm light at 0.5V bias voltage, the repeatability property(ON/OFF) with the sensitivity of UV detector for 8 *s*.

1613
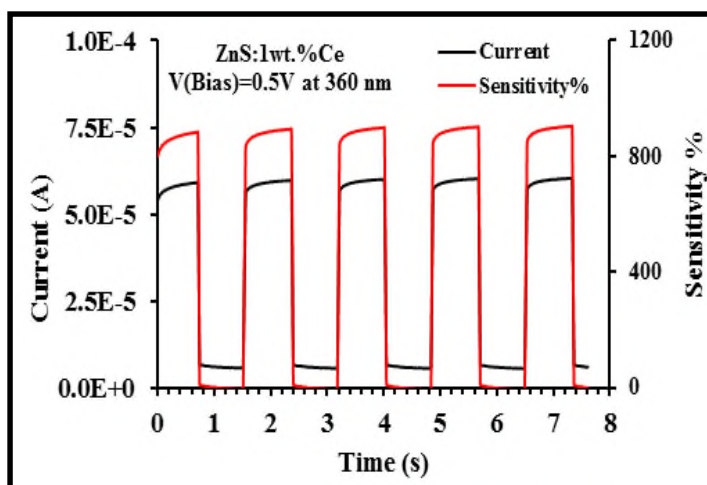
**Figure(7)Photoresponse time of the fabricated ZnS:1wt.%Ce QDs UV
photodetector upon exposure to 360 nm light at 0.5V bias voltage, the
repeatability property(ON/OFF) with the sensitivity of UV detector for 8 s**

**Table (2) Some parameters extracted from (I-t) measurements for Mn and Ce
doped ZnS at 0.5V bias voltage.**

Sample	Dark current (μA)	Photocurrent (μA)	$\mathfrak{t}_r$ (ms)	$\mathfrak{t}_f$ (ms)	Δf (Hz)	G	Sensitivity %
ZnS:Mn	35	158	49.79	47.44	25.3357	8.08	808
ZnS:Ce	14	93	38.81	24.62	40.8831	9.50	950

Figure of merit

Spectral photoresponses from doped ZnS devices were measured at fixed 0.5 V bias. All the measurements were performed at room-temperature and ambient environment. The photoresponsivity, quantum efficiency, Noise-Equivalent Power (NEP), Detectivity D and Specific Detectivity D* of photodetector devices can be estimated as follows:

(I) Responsivity R(λ) for ZnS PC Detector

The responsivity of the ZnS nanoparticles-based UV photodetector was obtained using the relation [15]: $R(\lambda) = I_{ph}(\lambda)/P_{inc}(\lambda)$ where I_{ph} is photocurrent and P_{inc} is incident UV light power, which is 61mW/cm².

The responsivity of the fabricated UV photoconductive detector; measured at 0.5 V applied bias voltage and 300 nm illumination with 61 mW/cm² light intensity; was 1.49 & 5.59 A/W for Mn doped ZnS & Ce doped ZnS UV photodetector respectively. The obtained responsivity of our device is more than those reported by Fang et al. [16] for ZnS nanobelt-based UV photodetectors which is 1x10⁻²⁶ A/W at 10 V bias voltage upon 320 nm light illumination.

The spectral responsivity of the fabricated UV photodetector is shown in Fig. 8. As shown in this figure, the photoresponsivity was high in the UV region (200 - 300 nm). High UV-to-visible rejection ratio can be defined as the responsivity measured at 300 nm divided by the responsivity at 450 nm [17].
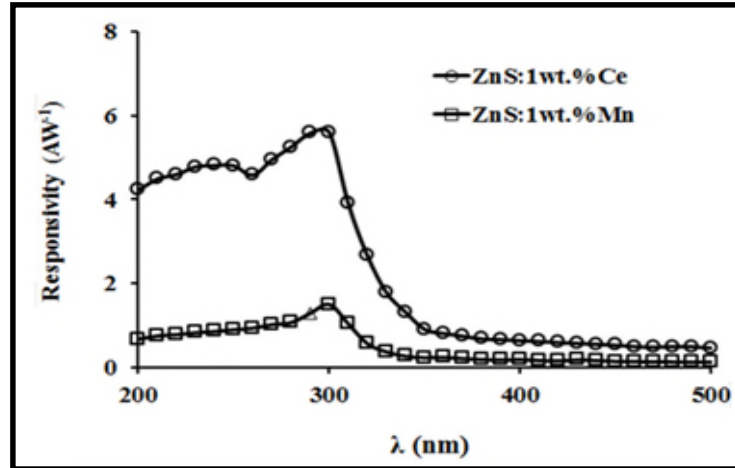

Figure (8) The variation of spectral responsivity with wavelength of ZnS:1wt.%Ce and ZnS:1wt.%Mn detectors at 0.5V bias voltage.

(II) Quantum Efficiency (QE) η(λ)

The quantum efficiency (QE) of the Mn and Ce doped ZnS QDs-based UV photodetector was obtained using the relation [15]:

$$\left[\, \eta(\lambda) = \frac{1240}{\lambda(nm)} \times R(\lambda) \times 100\% \,\right]$$, we can see that Mn doped ZnS device shows QE

of 620% in UV region (300 nm) and 0.5 V applied bias voltage. Furthermore, the device Ce doped ZnS shows an enhancement in UV-detection-gain 2310% by a factor of ~ 3.5. The results suggest that Ce doped ZnS device is most sensitive to UV light. The obtained QE of our devices is more than those reported by Liang et al. [18] for ZnS nanowire (R_λ of approximately 1.86 A W^{-1} and QE of approximately 7.1 × 10^2%). The QE of the fabricated UV photodetector is shown in Fig. 9.
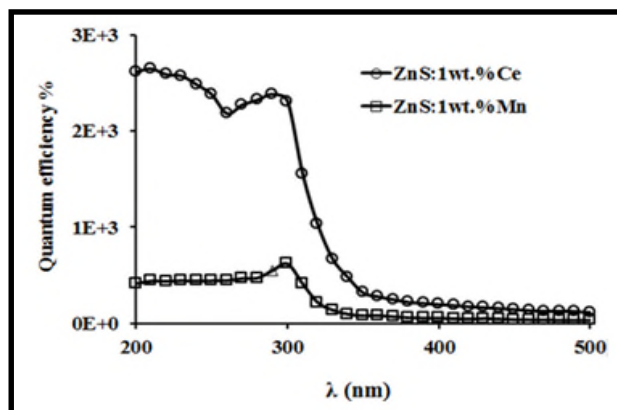

Figure (9) The variation of QE with wavelength of ZnS:1wt.%Ce and ZnS:1wt.%Mn detectors at 0.5V bias voltage

(III) Noise-Equivalent Power (NEP)

NEP of the ZnS nanoparticles-based UV photodetector was obtained using the relation [15]: $NEP = I_n/R_\lambda$ …(1)

where

I_n is noise current (If noise from the dark current is the dominant contribution) so noise current is given by:

$$I_n = \sqrt{4k_BT\Delta f/R_d}$$ …(2)

Where:

R_d is resistance of detector in the dark and Δf is bandwidth which is given by [15]:

$$[\tau_r = 2.2/(2\pi\Delta f) = 0.35/\Delta f]$$ …(3)

Where:

τ_r equals to . The detecting capability of the detector improves as the NEP decreases.

NEP of the fabricated UV photoconductive detector; measured at 0.5 V applied bias voltage and 300 nm illumination with 61 mW/cm² light intensity; was 1.93×10^{-12} W & 0.51×10^{-12} W for Mn doped ZnS & Ce doped ZnS UV photoconducive detector respectively. The NEP of the fabricated UV photodetector is shown in Fig. 10.
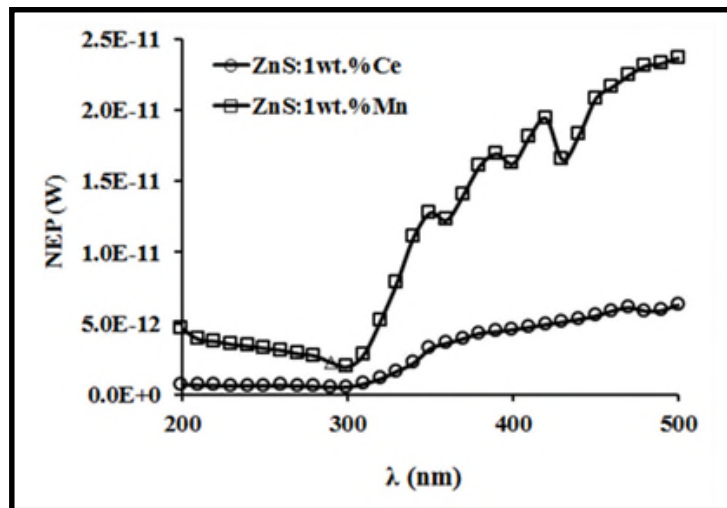
**Figure(10) The variation of NEP with wavelength of ZnS:1wt.%Ce and
ZnS:1wt.%Mn detectors at 0.5V bias voltage.**

(IV) Detectivity D & Specific Detectivity D*

The detectivity (D) and Specific Detectivity D* of the UV photodetector device is given by using the relations [15]: $[D = 1/NEP]$ and $\left[D^* = \sqrt{\Delta f.A_d}/NEP\right]$. Under illumination at 300 nm UV light, the calculated detectivities of Mn doped ZnS & Ce doped ZnS devices (with fixed 0.5 V bias) are 0.51×10^{12} W⁻¹ and 1.93×10^{12} W⁻¹ respectively as shown in figure 11. The specific detectivities of ZnS:1wt.%Mn & ZnS:1wt.%Ce devices are 0.73×10^{12} and 2.76×10^{12} Jones respectively. Specific detectivities of our devices are much higher compared to the detectivity of previously reported photodetectors based on inorganic ZnS hybrid system (10^{10} Jones) [16].
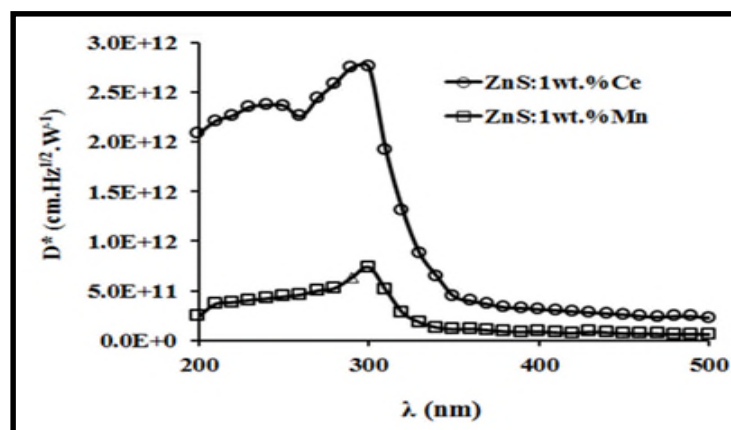
Figure (11) The variation of Specific Detectivity with wavelength of ZnS:1wt.%Ce and ZnS:1wt.%Mn detectors at 0.5V bias voltage.

Table (3) Figure of merit for ZnS:1wt.%Mn & ZnS:1wt.%Ce UV photodetector measured at 0.5 V bias and 300 nm illumination.

Device structure	$R(\lambda)$ (A/W)	UV-to-visible rejection ratio	QE (%) $\times 10^3$	NEP (W) $\times 10^{-12}$	D^* (Jones) $\times 10^{12}$
Pd/Mn doped ZnS/Pd	1.49	11.46	0.62	0.51	0.73
Pd/Ce doped ZnS/Pd	5.59	10.75	2.31	1.93	2.76

CONCLUSIONS

ZnS doped with manganese and cerium QDs with a cubic structure have been prepared successfully by a novel method using microwave irradiation. It is a simple and efficient method to produce ZnS nanoparticles with regular shape, small size and high purity. It has been fabricated a photoconductive detector successfully. The device can operate at low bias voltage under UV illumination and it can show highest sensitivity and very fast response making them having potential applications as electrical gating for binary switching. The photoresponse in ZnS:(Mn & Ce) is distinctively different from conventional semiconductor photon detectors whose photoresponse strongly depends on light wavelength and an efficiency of ~10^3% is achieved with a biased photodetector at 0.5 V. The fabrication method studied here opens a viable route to doped ZnS optoelectronics for fast and highly-efficient photoconductive detectors.

Acknowledgement

REFERENCES

[1] Rogach A. L., "Semiconductor Nanocrystal Quantum Dots: Synthesis, Assembly, Spectroscopy and Applications", Springer Wien New York, (2008).

[2] Dragoman M. and Dragoman D., "Nanoelectronics: Principles and Devices", 2nd ed. Artech House, (2009).

[3] Alivisatos P., "The use of nanocrystals in biological detection", Nature Biotechnology 22, 47-52 (2004).

[4] Callister J. and Malinowski S., "Optical Properties In Anderson", Materials Science and Engineering: An Introduction (6th). John Wiley & Sons, Inc.: New Jersey, 707–729 (2003).

[5] Mishra S. K., Srivastava R. K., Prakash S. G., Yadav R. S. and Panday A. C., "Photoluminescence and photoconductive characteristics of hydrothermally synthesized ZnO nanoparticles", Opto−Electronics Rev., 18, 467 (2010).

[6] Eman M. N., "Fabrication and Characterization of n-ZnS/p-Si and n-ZnS:Al/p-Si Heterojunction", Int. J. Engineering and Advanced Technology, 3(2) (2013).

[7] Sharma P., Sreenivas K. and Rao K. V., "Analysis of ultraviolet photoconductivity in ZnO films prepared by unbalanced magnetron sputtering", J. Appl. Phys., 93, 3963 (2003).

[8] Law J. B. and Thong J. T., "Simple fabrication of a ZnO nanowire photodetector with a fast photoresponse time", Appl. Phys. Lett., 88, 133114 (2006).

[9] Klein D. L., Roth R., Lim A. K., Alivisatos A. P., McEuen P. L., "A single-electron transistor made from a cadmium selenide nanocrystal", Nature , 389, 699-701 (1997).

[10] Gerberich, W. W., "Superhard silicon nanospheres", J. Mech. Phys. Solids 51, 979-992 (2003).

[11] Trindade, T., O'Brien, P., Pickett, N. L., "Nanocrystalline semiconductors: Synthesis, properties, and perspectives", Chem. Mater. 13, 3843-3858 (2001).

[12] Olkhovets A., Hsu R.C., Lipovskii A., Wise F.W., "Size-Dependent Temperature Variation of the Energy Gap in Lead-Salt Quantum Dots", Phys. Rev. Lett. 81, 3539-3542 (1998).

[13] Dong B, Cao L, Su G, Liu W, Qu H, Zhai H, "Water-soluble ZnS:Mn/ZnS core/shell nanoparticles prepared by a novel tow step method". J Alloy Compd 492, 363–367 (2010).

[14] Soci C., Zhang A., Xiang B., Dayeh S.A., Aplin D.P.R., Park J., Bao X.Y. and Wang D., "ZnO Nanowire UV Photodetectors with High Internal Gain", Nano Lett., 7, 1003-1009 (2007).

[15] Lui,J.M., "Photonic Devices", Cambridge University Press: Cambridge, 2005.

[16] Fang X. S., Bando Y., Liao M. Y., Zhai T. Y., Gautam U. K., "An efficient way to assemble ZnS nanobelts as ultraviolet-light sensors with enhanced photocurrent and stability", Adv. Funct. Mater,20, 500–8 (2010).

[17] Jiang D. Y., Zhang J. Y., Lu Y. M., Liu K. W., Shen D. Z., and Fan X. W., "Ultraviolet Schottky Detector Based on Epitaxial ZnO Thin Film", Solid-State Electron, 52, 679 (2008).

[18] Liang Y, Liang H, Xiao X, Hark S., "The epitaxial growth of ZnS nanowire arrays and their applications in UV-light detection**",** J. Mater Chem., **22,** 1199 (2012).